2023 IMEKO TC-4 International Conference on
Metrology for Archaeology and Cultural Heritage
Rome, Italy, October 19-21, 2023

Development of a Quantitative Multimodal Imaging Technique for In-situ Study of Iron Archaeological Artefacts

Granget Elodie[1], Cocen Ocson Reginald[1,4], Shakoorioskooie Mahdieh [2], Qianru Zhan [2,3], Lumongsod-Thompson Marian Nida[4], Kaestner Anders[2], Mannes David[2], Brambilla Laura[1]

[1] *Haute Ecole Arc Conservation-Restauration, HES-SO University of Applied Sciences and arts Western Switzerland, Espace de l'Europe 11, 2000 Neuchâtel, Switzerland, elodie.granget@he-arc.ch, ocson.cocen@he-arc.ch, Laura.brambilla@he-arc.ch*

[2] *Laboratory for Neutron Scattering and Imaging at the Paul Scherrer Institute, Forschungsstrasse 111, 5232 Villigen, Switzerland, mahdieh.shakoorioskooie@psi.ch, qianru.zhan@psi.ch, anders.kaestner@psi.ch, david.mannes@psi.ch*

[3] *Institute for Building Materials (IfB), ETH Zurich, 8093 Zürich, Switzerland*

[4] *Tribology and Interfacial Chemistry (TIC) Group, SCI-STI-SM, Institute of Materials, École polytechnique fédérale de Lausanne (EPFL), Station 12, 1015 Lausanne, Switzerland, marian.lumongsod@epfl.ch*

***Abstract* – This paper presents the methodology and preliminary results of the SNSF Sinergia project CORINT. The project aims to elucidate the corrosion phenomena of iron objects in various porous media, in particular iron archaeological artefacts (IAAs) in soil. A multimodal quantitative imaging technique, combining neutron and X-ray computed tomography (NX-CT), is being developed to study corrosion processes non-destructively. The methodology involves the registration and fusion of neutron and X-ray tomogram data, followed by segmentation using Gaussian mixture model (GMM) clustering. Two IAAs, with sample names Vrac C and BdC1, were imaged. Random cross-sections of these samples were also analyzed using optical microscopy, Raman spectroscopy, and SEM-EDS to characterize and cross-correlate the corrosion layers with the NX-CT results. This research provides insights into the corrosion state of IAAs and offers a non-destructive approach to studying corrosion processes in porous media. This will bring benefits to cultural heritage preservation, and to the study of the long-term corrosion behaviors of modern iron structures, steel in concrete, and nuclear waste disposal plans.**

I. INTRODUCTION

The SNSF Sinergia project – CORINT (project number CRII5_205883/1) engages partnerships between scientists from the Department of Materials Science and Engineering of the Swiss Federal Institute of Technology in Lausanne (EPFL SCI-STI-SM), the Department of Civil, Environment and Geomatic Engineering at the Swiss Federal Institute of Technology in Zürich (ETHZ BAUG), the Research Unit in Conservation-Restoration of the University of Applied Sciences Arc of Neuchâtel (HE-Arc) and the Laboratory for Neutron Scattering and Imaging at the Paul Scherrer Institute (PSI-LNS). The main goal of the CORINT project is to elucidate the corrosion phenomena of iron objects in various porous media. HE-Arc focuses on iron cultural objects in an archaeological context, i.e., objects embedded in soil.

Understanding the corrosion state of IAAs is crucial for developing appropriate conservation treatments and preservation plans [1]. However, IAAs have broader implications beyond cultural heritage. They are often used as analogues in studies investigating the long-term corrosion behaviors of modern iron structures and in the context of nuclear waste disposal plans [2, 3, 4, 5], as laboratory simulations have limitations in replicating real-world complexities developed during a time span of centuries or millennia. Numerous studies have examined IAAs under various conditions, such as exposure to the atmosphere [6, 7, 8, 9], burial in anoxic environments [10], presence in carbonate- or sulfide-rich soils [3, 5], and exposure to chloride [11]. These studies have proposed and refined corrosion mechanism models specific to each environment. However, they often required destructive analyses of actual IAAs, which is understandable from a research standpoint but not favored in heritage conservation practice and standards.

Hence, a multimodal quantitative imaging technique based on NX-CT is being developed through a close collaboration between all partners of the CORINT project. PSI and HE-Arc are working together to enable such analysis on IAAs. The goal is to perform non-destructive quantitative analysis and characterization of corrosion products by appropriately segmenting neutron and X-ray fused tomograms and labeling each identified corrosion layer. This segmentation and labeling process involves the use of traditional and invasive analytical techniques, which

results serve as a reference database during the development phase. Once the quantitative multimodal imaging is fully established, it will facilitate the documentation of the initial corrosion state of IAAs in their original surrounding soils. Moreover, it will help identify any changes that may have occurred during excavation, handling, conservation treatments, such as dichlorination [12], and storage.

II. MATERIALS AND METHODS

For the development of NX-CT, the chosen approach involves a sequential process of data fusion. Initially, neutron and X-ray tomograms are acquired at the PSI facility. Then those tomograms are registered together using an affine transform (SimpleElastix library [13]). The bivariate histogram of the registered images was used to segment the pixel values into 4 clusters, using a Gaussian mixture model (GMM). Only after being imaged, the objects were embedded in resin, cut, and at least four cross-sections of each sample were studied using optical microscopy (OM), µRaman, and SEM-EDX.

A. Selected objects

Vrac C and BdC1, two iron archaeological artefacts, were provided by the Roman Sites and Museum of Avenches (SMRA), Switzerland. Vrac C is a decontextualized nail that was found in the excavated soil pile by the detectorists alongside others. Since it wasn't attributed to any strata, it wasn't kept for extended study and was only partially micro-sandblasted to allow archaeologists to identify its shape. It was then stored in an unmonitored environment and showed signs of chloride presence in the remaining corrosion products. BdC1 is the first artefact sampled on-site for the CORINT project. It was extracted from the ground during a site survey and kept as a test sample for the NX-CT calibration, as it was already disturbed from its initial environment.

Table 1. Parameters for imaging

Beamline	Neutron exposure **(s)**	X-ray exposure (s)	X-ray energy (kV)	Projections	Pixel size **(µm)**	horizontal view field **(mm)**
ICON	80	10	150	1125	13.8	27
NEUTRA	100	20	250	625	34.4	66.6

B. Tomographies

The tomograms for the Vrac C were obtained using a micro-setup at the ICON beamline [14], which employs a cold neutron source. Conversely, the tomograms for BdC1 were acquired using a midi-setup at the NEUTRA beamline [15], employing thermal neutrons. The imaging parameters for X-ray and neutron imaging are detailed in Table 1.

C. Optical Microscopy and Raman spectroscopy

The OM images were acquired with a Zeiss microscope equipped with an Axiocam 305 color digital camera. Multiple views at 5x magnification are stitched together using Zeiss ZEN software.

The µRaman analyses were performed with the RENISHAW Virsa Raman analyzer and using WIRE 5 software. All spectra were acquired using a 785nm laser. The phases were isolated using a 20x to 50x magnification, depending on their size. Acquisitions were usually made using the following parameters: 1 second, 25-30 accumulations, and energy between 12-10 mW. The data was then processed with Spectragryph 1.2 software.

In addition to Raman spectroscopy, SEM-EDX analysis was performed using GeminiSEM 300 by Zeiss. SEM images (20kV, Everhart-Thornley secondary electron detector), EDS spectra (20kV, 20s) and EDS maps (20kV, 40-50s) were acquired and processed using Aztec software by Oxford Instruments.

III. RESULTS

This section exemplifies the workflow described above by providing the current results obtained from the analysis of Vrac C. Subsequently, the same data processing methodology has been successfully applied to BdC1, which presents a more complex case but aligns closely with the real-case scenarios. The latest results will be included in the conference's presentation.

A. CT imaging

Neutron and X-ray images were first reconstructed separately, registered, and segmented based on their bivariate histogram using the GMM clustering algorithm (Fig. 1). These layers are identified by differences in X-ray and/or neutron attenuation. At this step, the layers are not yet labeled.

To emulate the real-case undisturbed scenario where an archaeological object is still surrounded by its burial soil, BdC1 was reinserted in a 5cm diameter cylinder filled with soil.

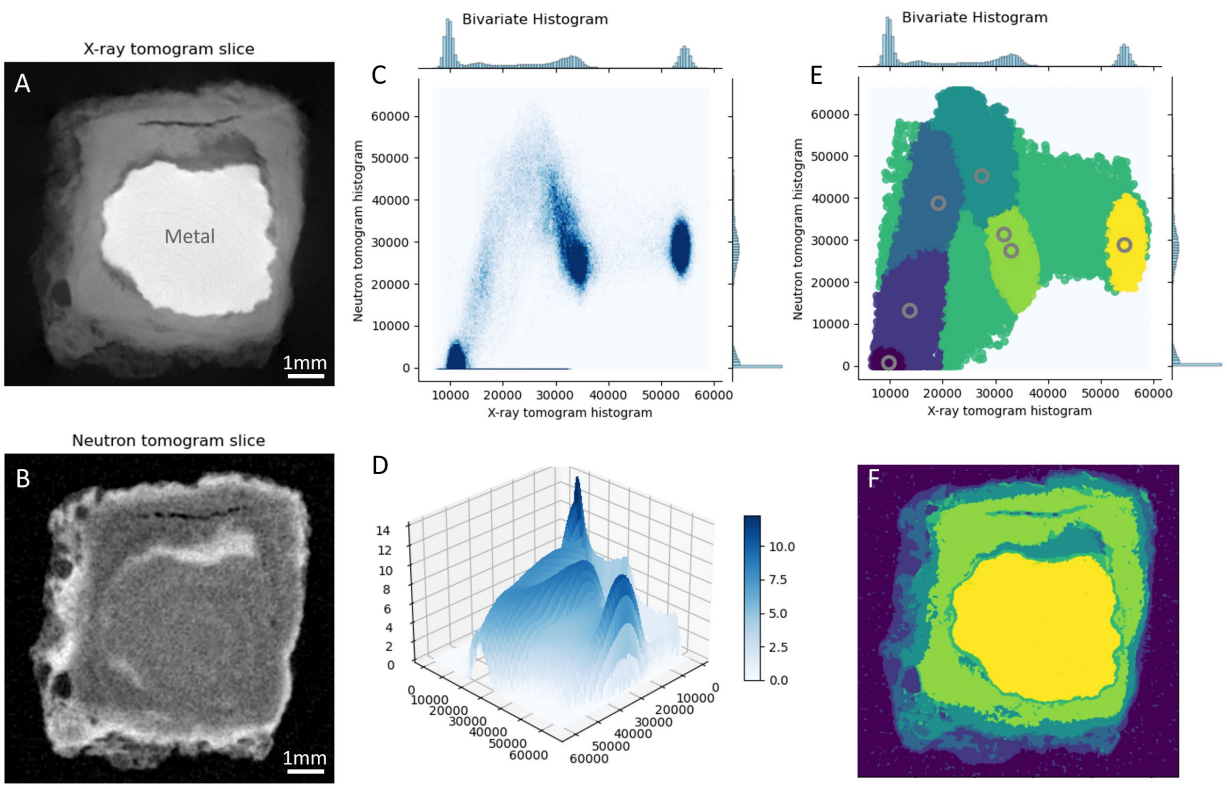

Fig. 1. Bimodal imaging and image segmentation results for Vrac C sample imaged using ICON instrument at PSI. A. X-ray tomogram slice; B. Neutron tomogram slice; C and D, two- and three-dimensional bivariate histograms of the pixel values based on X-ray and neutron tomograms; E. Clustered bivariate histogram using Gaussian Mixture Model (GMM) with specified priors (gray circles) based on expert opinion; F. Example map of color-coded segmented phases on the corresponding cross-section of the sample, as shown in insets A and B. ©CORINT_PSI

B. Investigation on cross-sections

Based on stitched OM images, layers of corrosion present in the objects were identified. Characterization of these phases was done using µRaman (Fig. 2). Further investigation with SEM-EDS has been undertaken when deemed necessary. This characterization protocol aims at identifying (labeling) the various layers that were detected and segmented in the NX-CT images and refining the clustering process, when it appears that some layers were missing or superfluous.

To be able to directly compare different phases between the non-destructive and destructive characterization results, at a specific cross-section of the objects, the OM images of each cross-section will be registered (2D to 3D registration) to the corresponding cross-section in the pixel based fused NX tomograms (NXF). The OM image also serves as the carrier of the labeled phases identified by Raman spectroscopy. In other words, the phase labels will be automatically registered and thus easily fused with the NXF. The same workflow will also be carried out between the NXF and SEM images (also serving as a carrier for EDX elemental analysis results). Taking multiple cross-sections allows for more accurate extrapolation throughout the tomograms. Ultimately, a multimodal fusion of NXF, OM, SEM-EDX, and Raman data will be performed. The fusion of NXF and OM plays a crucial role in the segmentation process. Subsequently, spectroscopy analysis is used to label each layer identified on the tomograms. These results are being processed and will also be included in the conference's presentation.

As a qualitative analysis (with no data fusion) for Vrac C, the three main strata, namely the Metal core (M), Dense Product Layer (DPL), and Transformed Medium (TM) as described in the literature [3] were identified (Fig. 3). Phases of the DPL could be analyzed with µRaman. TM caused more fluorescence during Raman analysis, making it harder to characterize. A complementary SEM-EDX analysis provided the layers' composition. These analyses revealed elements expected in the soil (Si, Al, Mg, K, Na) [16], mixed with iron oxides (Fig.4).

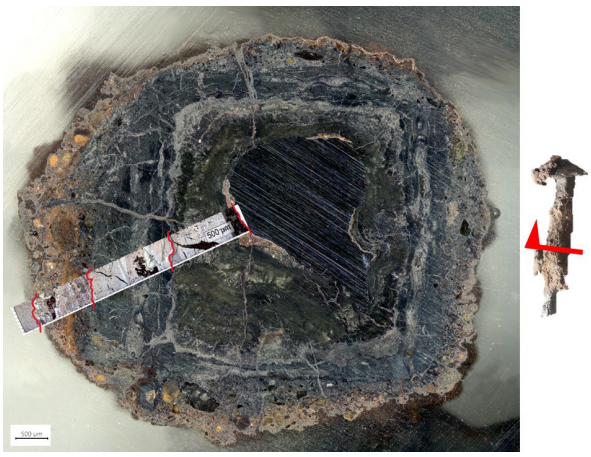

Fig. 2. Vrac C OM overview stitched image, with registered position of OM close-up of the zone analysed by µRaman spectroscopy and approximate location of the cross section Vrac C a. ©CORINT_HE-Arc

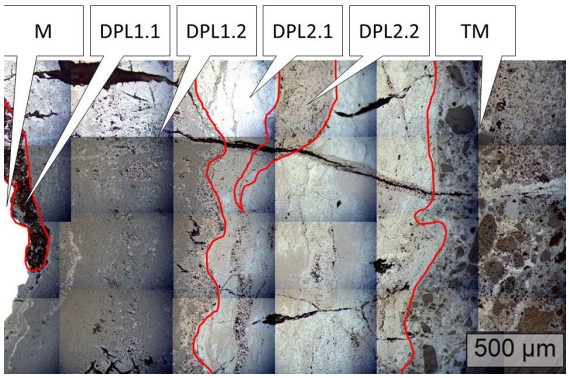

Fig. 3. Vrac C OM overview stitched image with main phases as identified with µRaman ©CORINT_HE-Arc

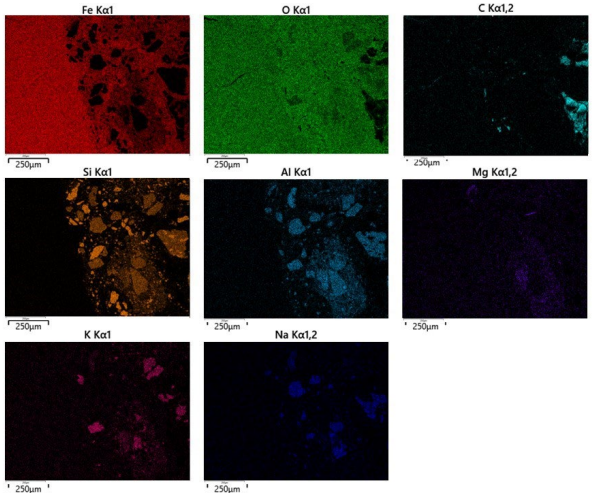

Fig. 4. EDS maps of DPL2 and TM interface. Fe, O, C (resin), Si, Al, Mg, K, Na. ©CORINT_EPFL

DPL could be split into two sub-layers of different nature. DPL1 is made of chukanovite (DPL1.1) (Fig.5) [17] with inclusions and reprecipitations of magnetite in fine cracks. It showed signs of rapid re-corrosion at the interface with M. The presence of not only Cl-, but also S-containing phases was confirmed with SEM-EDX mapping. (Fig.6). DPL2 showed intertwined phases of magnetite (DPL2.2) and mixes of magnetite and hematite (DPL2.1).

Moreover, all cross-sections investigated showed cracks running through all corrosion layers, with reprecipitation phases as expected based on the literature [18]. In this case, the reprecipitate was identified as magnetite (Fig.5). Cracking also occurred within DPL2, or at the transition between DPL1 and DPL2. Hence, clusters of DPL1 were found inside of DPL2. Based on Raman analysis, TM is mostly composed of a mixture of goethite and akaganeite with silicate-based sediments and granite.

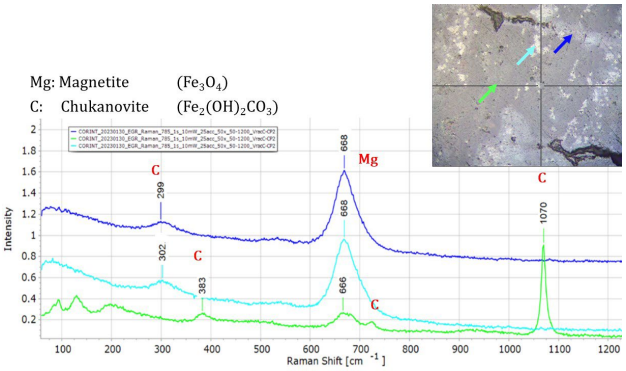

Fig. 5. Raman spectra of phases in DPL1.2 ©CORINT_HE-Arc

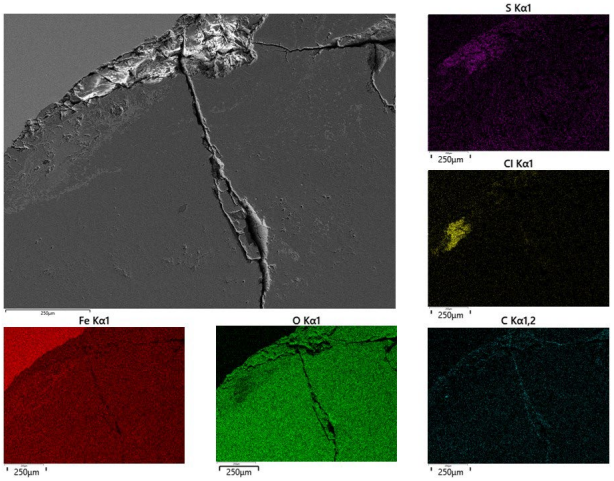

Fig. 6. EDS maps for DPL1.1 and DPL1.2. Fe, O, S, Cl, C (contaminants) ©CORINT_EPFL

IV. DISCUSSION

The registration process from Neutron and X-ray shows promising results. The required workflows for pixel-level fusion of the NX-CT data are being optimized at the moment and will soon be used to the fused NX tomograms.

The characterization of the DPL could be performed using Raman spectroscopy. Difficulties in obtaining good spectra with this technique on TM were solved by completing the analysis with SEM-EDX mapping. In the case of Vrac C, a nail from an urban site, a thick layer (~100-200 microns) of Cl-containing products was found in the DPL1. In the future, it will be interesting to compare these results to the one obtained on BdC1, an object found in a forest site.

The results of spectroscopic analyses and OM phase identification will be used to label different phases and refine their clustering using NXF.

The qualitative (and the planned accurate-quantitative) cross-referencing of the multi-modal data provides a comprehensive representation of the composition map of the layers identified in the tomograms. Such a reference table will serve as a crucial resource for future analyses, as it will enable accurate labeling of new tomograms and validation of the proposed method. Moreover, this approach paves the way for relying solely on tomography techniques in the future, still providing valuable insights on the nature of corroded iron objects but eliminating the need for destructive sample analyses.

V. CONCLUSION

In conclusion, the development of this multimodal quantitative imaging technique using NX-CT is well underway. This non-destructive approach, attempting the fusion of 3D, 2D, and spectral data, provides valuable insights into the corrosion state of IAAs and offers a promising method for studying corrosion processes in porous media prior to or without extraction from the environment itself.

The results obtained from the analysis of Vrac C demonstrated the effectiveness of the designed workflow. The fusion of neutron and X-ray tomograms enabled the segmentation of different corrosion layers based on clusters identified in their bivariant attenuation histograms. Optical microscopy, Raman spectroscopy, and SEM-EDS analysis further contributed to the characterization and labeling of these layers. The developed reference table and the correlation between spectroscopic data and tomographic intensities provide a comprehensive representation of the composition of the identified layers. Moving forward, additional data from pure corrosion compounds of iron will be analyzed following the same workflow, and the resulting data will be added to the reference table. This will further enhance the accuracy of phase identification and labeling in the tomograms. Ongoing collaboration between the project partners and the continuous refinement of the multimodal imaging technique will break ground for relying solely on tomography techniques in the future, thus offering a non-destructive yet comprehensive approach to studying corrosion processes, that at the same time aligns well with heritage conservation standards. From these results, conservators and scientists can develop appropriate conservation treatments, preservation plans, and corrosion mitigation strategies for various applications.

Moreover, the insights gained from the CORINT project will contribute not only to the preservation of cultural heritage objects but also to academia and the materials science industries.

VI. CITATIONS AND REFERENCES

[1] Selwyn, L. "Overview of archaeological iron: The corrosion problem, key factors affecting treatment, and gaps in current knowledge." Metal 04: Proceedings of the International Conference on Metals Conservation. 2004

[2] Miller, W. Varieties of analogue studies. Geological Disposal of Radioactive Wastes and Natural Analogues. R. A. William Miller, Neil Chapman, Ian Mckinlely, John Smellie, Pergamon. 2: 53-63. 2000

[3] Neff D, Dillmann P, Bellot-Gurlet L, Beranger G. Corrosion of iron archaeological artefacts in soil: characterisation of the corrosion system. Corros Sci. 2005.

[4] Chitty WJ, Dillmann P, L'Hostis V, Lombard C. Long-term corrosion resistance of metallic reinforcement in concrete—a study of corrosion mechanisms based on archaeological artefacts. Corros Sci. 2007.

[5] Rémazeilles C, Neff D, Bourdoiseau JA, Sabot R, Jeannin M, Refait P. Role of previously formed corrosion product layers on sulfide-assisted corrosion of iron archaeological artefacts in soil. Corros Sci. 2017.

[6] Dillmann P, Mazaudier F, Hoerlé S. Advances in understanding atmospheric corrosion of iron. I. Rust characterisation of ancient ferrous artefacts exposed to indoor atmospheric corrosion. Corros Sci. 2004

[7] Hoerlé S, Mazaudier F, Dillmann P, Santarini G. Advances in understanding atmospheric corrosion of iron. II. Mechanistic modelling of wet-dry cycles. Corros Sci. 2004.

[8] Monnier J, Burger E, Berger P, Neff D, Guillot I, Dillmann P. Localisation of oxygen reduction sites in the case of iron long term atmospheric corrosion. Corros Sci. 2011.

[9] Monnier J, Neff D, Réguer S, Dillmann P, Bellot-Gurlet L, Leroy E, Foy E, Legrand L, Guillot I. A corrosion study of the ferrous medieval reinforcement of the Amiens cathedral. Phase characterisation and localisation by various microprobes techniques. Corros Sci. 2010.

[10] Mercier-Bion F, Li J, Lotz H, Tortech L, Neff D, Dillmann P. Electrical properties of iron corrosion layers formed in anoxic environments at the nanometer scale. Corros Sci. 2018.

[11] Réguer S, Dillmann P, Mirambet F. Buried iron archaeological artefacts: corrosion mechanisms related to the presence of Cl-containing phases. Corros Sci. 2007.

[12] Jacot-Guillarmod, M., Schmidt-Ott, K., Mannes, D. et al. Multi-modal tomography to assess dechlorination treatments of iron-based archaeological artifacts. Herit Sci 7, 29. 2019.

[13] Marstal, K. Berendsen, F. Staring M. and Klein, S. SimpleElastix: A User-Friendly, Multi-lingual Library for Medical Image Registration, 2016 IEEE Conference on Computer Vision and Pattern Recognition Workshops (CVPRW), Las Vegas, NV, USA, 2016, pp. 574-582.

[14] Kaestner, A.P., Hartmann, S., Kühne, G., Frei, G., Grünzweig, C., Josic, L., Schmid, F., Lehmann, E.H. The ICON beamline – A facility for cold neutron imaging at SINQ, Nuclear Instruments and Methods in Physics Research Section A: Accelerators, Spectrometers, Detectors and Associated Equipment,Volume 659, Issue 1,2011, Pages 387-393.

[15] Lehmann, E. H., Vontobel, P., Wiezel, L. Properties of the Radiography Facility NEUTRA at SINQ and its Potential for Use as European Reference Facility, Nondestructive Testing and Evaluation, 16:2-6, 2001, p. 191-202.

[16] Sposito, G. Geochemistry in Soil Science. In: Chesworth, W. (eds) Encyclopedia of Soil Science. Encyclopedia of Earth Sciences Series. Springer, Dordrecht. 2008.

[17] Michelin, A. Long term alteration of glass/iron systems in anoxic conditions: contribution of archaeological analogues to the study of mechanisms. Thesis. Science des matériaux. Université Pierre et Marie Curie - Paris VI, 2011. p. 145

[18] Grevey, AL., Vignal, V., Krawiec, H. et al. Microstructure and long-term corrosion of archaeological iron alloy artefacts. Herit Sci 8, 57 2020.